Published in final edited form as:
NanoImpact. 2018 July ; 11: 156–163. doi:10.1016/j.impact.2018.08.003.

Shifts in N and $\delta^{15}N$ in wheat and barley exposed to cerium oxide nanoparticles

Cyren M. Rico[a,b,d,*,†], **Mark G. Johnson**[b], **Matthew A. Marcus**[c], and **Christian P. Andersen**[b]

[a]National Research Council, Research Associateship Program, 500 Fifth Street, NW, Washington, DC 20001, USA

[b]US Environmental Protection Agency, National Health and Environmental Effects Research Laboratory, Western Ecology Division, 200 SW 35th St., Corvallis, OR 97333, USA

[c]Advanced Light Source, Lawrence Berkeley National Laboratory, 1 Cyclotron Road, Berkeley, CA 94720, USA

[d]Missouri State University, Department of Chemistry, 901 S National Ave., Springfield, MO 65897, USA

Abstract

The effects of cerium oxide nanoparticles (CeO_2-NPs) on $^{15}N/^{14}N$ ratio ($\delta^{15}N$) in wheat and barley were investigated. Seedlings were exposed to 0 and 500 mg CeO_2-NPs/L (Ce-0 and Ce-500, respectively) in hydroponic suspension supplied with NH_4NO_3, NH_4^+, or NO_3^-. N uptake and $\delta^{15}N$ discrimination (i.e. differences in $\delta^{15}N$ of plant and $\delta^{15}N$ of N source) were measured. Results showed that N content and ^{15}N abundance decreased in wheat but increased in barley. Ce-500 only induced whole-plant $\delta^{15}N$ discrimination (−1.48‰, $P \leq 0.10$) with a simultaneous decrease ($P \leq 0.05$) in whole-plant $\delta^{15}N$ (−3.24‰) compared to Ce-0 (−2.74‰) in wheat in NH_4^+. Ce-500 decreased ($P \leq 0.01$) root $\delta^{15}N$ of wheat in NH_4NO_3 and NH_4^+ (3.23 and −2.25‰, respectively) compared to Ce-0 (4.96 and −1.27‰, respectively), but increased ($P \leq 0.05$) root $\delta^{15}N$ of wheat in NO_3^- (3.27‰) compared to Ce-0 (2.60‰). Synchrotron micro-XRF revealed the presence of CeO_2-NPs in shoots of wheat and barley regardless of N source. Although the longer-term consequences of CeO_2-NP exposure on N uptake and metabolism are unknown, the results clearly show the potential for ENMs to interfere with plant metabolism of critical plant nutrients such as N even when toxicity is not observed.

Keywords

environmental engineered nanomaterial; isotope; nitrogen; synchrotron micro-XRF

[*]Corresponding author. Tel: 417 836 3304; Fax: 417 836 5507; CyrenRico@MissouriState.edu (C. M. Rico).
[†]This research project was started at US EPA and finished at Missouri State University. The experimental part and N and $\delta^{15}N$ analysis were performed at US EPA while synchrotron analysis was performed when the first author moved to Missouri State University.

1. Introduction

Engineered nanomaterials (ENMs) are being used in a wide array of consumer products. The vast majority of ENM studies have examined the acute toxicity of nanoparticles and particle forms to determine if they represent a risk to human health and/or the environment (Servin and White, 2016; Zuverza-Mena et al., 2017). In studies that examined the effects of metal oxide nanoparticles on plants, most studies have shown low to moderate toxicity, even at relatively high ENM concentrations (Servin and White, 2016). However, release of ENMs into the environment may have other subtle effects on plant uptake and use of important nutrients, which could alter growth and development. For example, nitrogen is one of the most important nutrients since it is an essential component of amino acids, proteins and nucleic acids, including the carboxylating enzyme involved in photosynthesis (Tamm, 1991). Although many forms of N occur in soils, not all forms are available to plants. In addition, microbial processing of N affects pools and fluxes of N in soils. Understanding the effects of ENMs on factors such as N uptake and metabolism is important not only to understand plant growth and development, but also for understanding how ENMs may affect ecosystem processes.

Different isotopes of N have been used as sensitive indicators of metabolic change and also reflect shifts in ecosystem processing of N (Banas et al., 2009; Marshall et al., 2007). The $^{15}N/^{14}N$ ratio of plant tissue can be used to follow changes in response to both natural and environmental stresses, and often reflects discrimination against the heavier ^{15}N isotope compared to the lighter ^{14}N isotope (Craine et al., 2015; Kalcsits et al., 2014; Unkovich, 2013). Isotopic composition ($\delta^{15}N$) is expressed as

$$\delta^{15}N(‰) = \left(\frac{R_{sample}}{R_{standard}} - 1\right) \times 1000$$

where R_{sample} is the $^{15}N/^{14}N$ ratio of the sample and $R_{standard}$ is the ratio of known standard. The standard for nitrogen is atmospheric nitrogen ($^{15}N/^{14}N = 0.0036765$) (Craine et al., 2015; Kalcsits et al., 2014; Unkovich, 2013). Nitrogen isotope discrimination occurs when ^{14}N is utilized more readily than ^{15}N, resulting in lower and more negative $\delta^{15}N$ of plants ($\delta^{15}N_p$) than $\delta^{15}N$ of inorganic N source ($\delta^{15}N_s$). Figure A.1 summarizes nitrogen isotope discrimination in plants (Evans et al., 1996, 2001; Kalcsits et al., 2014; Kalcsits and Guy, 2013; Mariotti et al., 1982). According to this model, isotope discrimination is a function of influx of $(N)_{inorg}$ from N source, assimilation by root enzymes (i.e. nitrate reductase and glutamine synthetase) yielding ^{15}N-enriched $(N)_{inorg}$ and ^{15}N-depleted $(N)_{org}$, efflux of unassimilated ^{15}N-enriched $(N)_{inorg}$, and xylem transport of $(N)_{inorg}$ to the shoots (Evans et al., 1996, 2001; Kalcsits et al., 2014; Kalcsits and Guy, 2013; Mariotti et al., 1982).

Kalcsits et al. (2014) also noted that nitrogen isotope discrimination is largely a function of supply of root $(N)_{inorg}$ relative to the plant's demand for $(N)_{org}$. When there is no loss of root $(N)_{inorg}$ prior to assimilation, discrimination will not occur because the entire root $(N)_{inorg}$ will be converted to $(N)_{org}$. Whole-plant $\delta^{15}N$ discrimination (i.e. differences between $\delta^{15}N_p$ and $\delta^{15}N_s$) occurs if fractionation occurs during influx or efflux occurs from unassimilated ^{15}N-enriched $(N)_{inorg}$. Organ-level discrimination (i.e. difference between root and shoot

$\delta^{15}N$ and $\delta^{15}N_s$) is mainly the function of efflux of root $(N)_{inorg}$, and xylem transport of $(N)_{inorg}$ and ^{15}N-depleted $(N)_{org}$ to the shoots (Evans et al., 2001; Kalcsits et al., 2013, 2014).

Previous studies showed the impacts of heavy metal on N metabolism in plants, and it is possible that metal oxide nanoparticles could influence N uptake. Sutter et al. (2012) reported that Cd, Pb, and Zn decreased ^{15}N abundance in aquatic moss (*Fontinalis antipyretica* L. ex Hedw.) while Schmidt et al. (2004) found that As(III) or As(V) significantly decreased ^{15}N incorporation in *Silene vulgaris*. These researchers found that metals affected N uptake and protein synthesis which resulted in decreased metabolic activity of plants. We also reported decreases in $^{15}N/^{14}N$ ratio of wheat treated with cerium oxide nanoparticles (CeO_2-NPs), but did not find whether the isotopic changes occurred in the soil, the root rhizosphere, or after N uptake through changes in root or shoot metabolism (Rico et al., 2017).

In order to help isolate the mechanisms underlying changes in N uptake and/or metabolism in response to ENM exposure, we used hydroponic systems to allow us to control the forms and isotopic ratios of N supplied to the roots, and to minimize the influence of soil interactions external to plant roots. We selected CeO_2-NPs since they are widely used in many technological applications that could reach the environment and interact with terrestrial/agricultural plant species (Dahle and Arai, 2015). In this study, the influence of CeO_2-NPs on nitrogen metabolism of different forms of N (i.e. NH_4NO_3, NH_4^+, NO_3^-) in wheat (*Triticum aestivum* L.) and barley (*Hordeum vulgare* L.) was explored. The hypotheses were 1) CeO_2-NPs do not alter uptake of N or growth in wheat and barley regardless of the form of N supplied, i.e., NO_3^-, NH_4^+ or NH_4NO_3, 2) shifts in the isotopic ratios of N in leaves and roots in response to the different forms of N supplied are not influenced by CeO_2-NPs exposure, and 3) wheat and barley show similar isotopic ratios in response to the different N forms and to CeO_2-NP exposure. We chose to study N because CeO_2-NPs modified N and ^{15}N abundance in wheat (Rico et al., 2017), and we chose wheat and barley because these species vary in response to CeO_2-NPs exposure, possibly indicating different modes of action (Rico et al., 2014, 2015a). We tested 500 mg CeO_2-NPs/L because this exposure level in soil altered roots, shoots, and grains $\delta^{15}N$ in wheat (Rico et al., 2017).

2. Materials and methods

2.1 Experimental design

This study was performed using the same CeO_2-NPs (Meliorum Technologies, Rochester, NY) previously used in wheat (Rico et al., 2014, 2015a, 2017). The CeO_2-NPs have been characterized as rods with primary size of 67±8 × 8±1 nm, particle size of 231±16 nm in DI water, surface area of 93.8 m^2/g, and 95.14% purity (Keller et al., 2010). A 10-day hydroponic experiment was performed using 0 and 500 mg CeO_2-NPs/L (Ce-0 and Ce-500, respectively) at three different N sources: ammonium nitrate (NH_4NO_3), ammonium alone (NH_4^+), and nitrate alone (NO_3^-). Unmodified Yoshida nutrient solution (Yoshida et al., 1976) was used for the ammonium nitrate experiment. For ammonium or nitrate alone experiments, the amount of N in ammonium nitrate was replaced with equal molar

concentrations of $NH_4Cl/(NH_4)_2SO_4$ or $KNO_3/Ca(NO_3)_2$. The experiment had six treatment combinations with six replicates for each treatment.

2.2 Plant cultivation and management

The nanomaterial suspensions were prepared as previously described in Rico et al. (2017). The nutrient solution (100 mL) was placed in 150-mL plastic jars (Nalgene, Rochester, NY). CeO_2-NPs were added to the solution then sonicated for 30 mins at 20^{o}C with occasional stirring. After sonication, the jars were covered with caps that had three holes where cuttings from 3 mL plastic pipette were fitted to hold two plants and air pumps (Aqua Supreme Air Pump, Petco). Air was constantly supplied using air pumps. All materials used for the hydroponic experiment were sterile and soaked in 10% hypochlorite solution before use. Two nine-day-old wheat or seven-day-old barley seedlings were grown in nutrient solution in growth chamber (Environmental Growth Chamber, Chagrin Falls, OH) set at 16-h photoperiod, 20/10˚C, 70% humidity, 300 μmol/m^2-s. At harvest, root and shoot were separated, washed thoroughly with Milli-Q water. After drying in the oven, total biomass was measured. Plant materials were ground and subjected to N and ^{15}N analysis.

2.3 Analysis of δ^{15}N

The analysis of N and δ^{15}N was performed using an Elementar Vario Isotope Cube (Elementar Analysensysteme GmbH, Hanau, Germany) interfaced to a Isoprime 100 isotope ratio mass spectrometer (Isoprime Ltd, Stockport UK) as described in Rico et al. (2017) Three laboratory isotope standards were analyzed to assess quality assurance or check calibration. The final values were expressed relative to Air as internal standard. The δ^{15}N values (‰) of the N source were: NH_4NO_3 (4.98±0.18), NH_4^+ (−1.76±0.61), and NO_3^- (3.21±0.25). Whole-plant δ^{15}N was calculated according to Robinson et al. (2000) as shown below. Whole-plant δ^{15}N discrimination occurs when whole-plant δ^{15}N is statistically lower than δ^{15}N of the N source ($\delta^{15}N_s$). Similarly, root or shoot δ^{15}N discrimination occurs when root or shoot δ^{15}N is statistically lower than $\delta^{15}N_s$.

$$Whole\ \ plant\ \ \delta^{15}N\ \ (‰) = \frac{\left(Shoot\ \ \delta^{15}N\ \ \times Shoot\ \ N\right) + \left(Root\ \ \delta^{15}N\ \ \times Root\ \ N\right) + \left(Grain\ \ \delta^{15}N\ \ \times Grain\ \ N\right)}{Shoot\ \ N\ \ + \ \ Root\ \ N\ \ + \ \ Grain\ \ N}$$

2.4 Synchrotron micro-XRF and micro-XANES analysis

Wheat and barley shoots were harvested at the end of the experiment. The shoots were washed thoroughly with Milli-Q water, flash-frozen in liquid nitrogen, and kept at −80°C. The frozen young leaves (~2.5 cm from the tip) were mounted, using a tiny amount of silicone grease, onto a Peltier stage and kept at −27°C to reduce radiation damage (Freeman et al., 2006). The μ-X-ray fluorescence (μXRF) and μ-X-ray absorption near edge structure (μXANES) analysis of Ce at the L_{III} edge in the frozen leaves was performed at 10.3.2 X-ray microprobe beamline at the Advanced Light Source (ALS) at Lawrence Berkeley National Laboratory following the method in Rico et al. (2017, 2018). The maps were collected with a 12(H)×6(V) μm^2 beam at 15×15 μm^2 pixel size and 50 ms dwell time at 5873eV. Energy

calibration was such that the first peak for CeO_2 was at 5730.39 eV. Cerium L_{III}-edge μXANES spectra were collected at points of interest based on the apparent presence of Ce at these locations as determined by the μXRF chemistry maps collected on shoots. Pre- and post-edge normalization and least squares combination fitting (LCF) were performed with ALS BL10.3.2 software. The fractions of Ce in Ce(III) and Ce(IV) forms at each spot was determined from the fitting results. Reference standard μXANES spectra for LCF analysis were those reported in Rico et al. (2018). Additional description of the methods was presented in Appendix B.

2.5 Data analysis

Statistical analyses were performed using SAS statistical package (SAS Institute, Cary, NC, USA). Two-way ANOVA was performed separately for wheat and barley. CeO_2-NPs (CE) was the main factor with Ce-0 and Ce-500 as the treatments while N source (NS) was another factor composed of NH_4NO_3, NH_4^+, and NO_3^- treatments. Whole-plant or organ-level (root or shoot) $\delta^{15}N$ discriminations were calculated. Statistical differences between $\delta^{15}N$, biomass, N concentration, N contents at Ce-0 and Ce-500 plants were also analyzed. Global mean N and $\delta^{15}N$ were calculated to measure effects of CeO_2-NPs across different N sources.

3. Results

3.1 Treatment effects and global mean calculations

The table of two-way ANOVA with CE (CeO_2-NPs treatments) and NS (N source) as main factors is presented in Appendix C (Tables C.1 and C.2). For wheat, NS was significant for all parameters measured while CE was significant only for every biomass, N contents, and $\delta^{15}N$ measurements (Table C.1). In barley, NS was also significant for all parameters except root N concentration, whereas CE was significant only for total shoot and plant N contents, root N concentration, and root $\delta^{15}N$ (Table C.2). The global mean of CE (mean across different N sources) were calculated and presented in Table 1. Ce-500 did not affect N concentration but decreased biomass, and all N contents and $\delta^{15}N$ in wheat, but increased global mean shoot and plant N, root N concentration, and root $\delta^{15}N$ in barley.

3.2 Changes in biomass, N concentration, and total N content between Ce-0 and Ce-500 plants are dependent on N source

In wheat, CeO_2-NPs only affected biomass production when NH_4NO_3 was used as the N source (Table 2). Ce-500 decreased both root and shoot dry weights (22 and 95 mg, respectively) compared to Ce-0 (40 and 123 mg, respectively). These decreases resulted in consistently lower root, shoot, and total N contents in Ce-500 (563, 2155, and 4393 μg, respectively) compared to the control (1001, 3055, and 4607 μg, respectively) (Figures 1A, C and E). Differences in N concentrations between Ce-0 and Ce-500 were not statistically significant (Table 1), but Ce-500 increased shoot and total N contents compared to Ce-0 in NH_4^+. Ce-500 also had higher shoot N content in NO_3^- compared to Ce-0 (Figure 1C).

For barley, significant differences between Ce-0 and Ce-500 treated plants were only observed in NH_4^+ (Table 1): root biomass increased at Ce-500 (10 mg) compared to Ce-0 (7

mg) while root N concentration (2.93%) decreased and shoot N concentration (2.75%) increased at Ce-500 relative to control (3.38% and 2.31%, respectively). However, N contents were much higher in the Ce-500 treatment than in Ce-0 controls in NH_4^+ (Figures 1B, D and F). Ce-500 also increased root and shoot N contents in the NH_4NO_3 treatment (Figures 1B and D).

3.3 Ce-500 modifications in whole-plant and organ $\delta^{15}N$ are N source dependent

For wheat, Ce-0 and Ce-500 induced whole-plant $\delta^{15}N$ discrimination (i.e. $\delta^{15}N$ of whole-plant was lower than the source) in NH_4NO_3 (Figure 2A). However, only Ce-500 in NH_4^+ resulted in whole-plant $\delta^{15}N$ discrimination (−1.48‰) with a simultaneous decrease in whole-plant $\delta^{15}N$ (−3.24‰) compared to the Ce-0 control (−2.74‰) (Figure 2C). In barley, the only shift observed was that Ce-500 had higher whole-plant $\delta^{15}N$ (4.96‰) than Ce-0 (3.88‰) when NH_4NO_3 was the N source (Figure 2B).

Figure 3 displays the effects of CeO_2-NPs on $\delta^{15}N$ discriminations (i.e. $\delta^{15}N$ of shoot was lower than the source) at the organ level. In wheat, Ce-500 induced root $\delta^{15}N$ discriminations in NH_4NO_3 and NH_4^+ (−1.74‰ and −1.69‰, respectively) (Figures 3A and C). In barley, discrimination against ^{15}N was not observed. Instead, Ce-500 increased root $\delta^{15}N$ in NH_4NO_3 and NO_3^- (0.86‰ and 1.29‰, respectively) compared to Ce-0 (Figures 3B and F).

Results also revealed significant differences in root and shoot $\delta^{15}N$ between Ce-0 and Ce-500 treated plants. For wheat in NH_4NO_3 and NH_4^+, Ce-500 decreased root $\delta^{15}N$ (3.23 and −2.25‰, respectively) compared to Ce-0 (4.96 and −1.27‰, respectively), but in NO_3^- Ce-500 increased root $\delta^{15}N$ (3.27‰) compared to the Ce-0 treatment (2.60‰) and to a level that root and shoot $\delta^{15}N$ (3.27‰ and 3.16‰, respectively) were statistically (Figures 3A, C, and E). In barley, statistical differences were observed in NO_3^- only: Ce-500 increased shoot $\delta^{15}N$ (4.62‰) compared to Ce-0 (3.61‰) (Figure 3B).

3.4 In-situ imaging of CeO_2-NPs in plant shoots

The synchrotron micro-XRF images revealed the presence of CeO_2-NPs in the shoots of wheat and barley at different N sources (Figure 4). The micro-XANES analysis showed that Ce was present in greater amount as CeO_2 (80–93%) and Ce(IV) to Ce(III) reduction (7–19%) occurred to a much lesser extent (Figure 4, Table D.1).

4. Discussion

Our results led to rejection of all three hypotheses tested in this study. N uptake and metabolism plays a central role in all cellular functions in plants, and the shifts observed here in response to CeO_2-NP exposure indicate that ENMs have the potential to alter how important nutrients such as N are utilized in plants, even when toxicity is not evident. Our hydroponic experiments removed the chemical and biological complexity of interactions that occur at the root-soil interface in soils in order to better understand possible mechanisms underlying changes in N uptake and metabolism in the two species. Additional studies will be needed to examine CeO_2-NP and N interactions in soil-grown plants, and to evaluate the longer-term consequences of changes in N dynamics in plants exposed to CeO_2-NPs.

4.1 Effects of CeO_2-NPs on N metabolism in wheat

CeO_2-NPs did not affect the root influx of $(N)_{inorg}$ from NH_4^+ since total plant and shoot N contents increased without changes in biomass and N concentration (Table 2, Figure 1C and E). However, the very high whole-plant and shoot $\delta^{15}N$ discriminations (i.e. $\delta^{15}N$ of whole-plant and shoot was lower than the source) in Ce-500 coupled with its low root $\delta^{15}N$ compared to Ce-0 strongly suggest low influx of ^{15}N into the roots or high efflux of ^{15}N-enriched $(N)_{inorg}$ to outside roots (Figure A.1). A previous study showed that discrimination in NH_4^+ uptake could result from efflux of ^{15}N-enriched NH_4^+ from $(N)_{inorg}$ (Figure A.1) (Evans et al., 1996). This could happen when NH_4^+ gets assimilated immediately in the roots which increases the pool of ^{15}N-enriched NH_4^+, then the ^{15}N-enriched NH_4^+ are transported out of the roots. Due to its toxicity, NH_4^+, generally is rapidly assimilated or flushed out of the roots (Evans et al., 1996).

In contrast, data seem to suggest that CeO_2-NPs decreased root to shoot translocation of ^{15}N (either T_o or T_i in Figure A.1) when the wheat seedlings were grown in NO_3^- because root $\delta^{15}N$ increased to similar level with shoot $\delta^{15}N$ despite decreased shoot N content and a lack of net change in whole-plant $\delta^{15}N$ discrimination (Figure 1C, 2E, 3E).

Wheat was a good discriminator of ^{15}N when the N source was NH_4NO_3 as shown by notable whole-plant and shoot $\delta^{15}N$ discriminations in Ce-0. Exposure to CeO_2-NPs only increased root $\delta^{15}N$ discrimination despite remarkable decreases in biomass production and N content. The decrease in root $\delta^{15}N$ was probably due to the discrimination against ^{15}N similar to what was observed in wheat in NH_4^+. It is also probable that shoot $\delta^{15}N$ from Ce-0 and Ce-500 was from $\delta^{15}N$ of the source NO_3^-, and the decrease root $\delta^{15}N$ was due to discrimination against ^{15}N from NH_4^+. Previous reports also showed that lower N uptake decreased ^{15}N abundance in Cd-treated aquatic moss (Sutter et al., 2002). In another report, alfalfa plants that exhibited impaired growth features when subjected to high carbon dioxide concentration and water deficiency had negative leaf $\delta^{15}N$ values (Ariz et al., 2015). In this study, N concentration in both shoot and root did not differ between Ce-500 and Ce-0 indicating that CeO_2-NPs did not affect N uptake and that reduced total N content was due to low plant biomass. It is possible that low biomass was due to reduction in macromolecules such as fatty acids and lignins similar to what was observed in rice seedlings exposed to CeO_2-NPs (Rico et al., 2013).

4.2 Effects of CeO_2-NPs on N metabolism in barley

In contrast to what was observed in wheat, CeO_2-NPs did not interfere with ^{15}N incorporation in barley and even increased whole-plant and organ $\delta^{15}N$, signifying that root $(N)_{inorg}$ in Ce-500 plants was converted to $(N)_{org}$ and efflux of ^{15}N-enriched $(N)_{inorg}$ did not occur. We believe this is consistent with the mechanism in Figure A.1 since the data showed that Ce-500 increased $\delta^{15}N$ values, especially in NH_4NO_3 and NO_3^-, without the increase in N content. Previous studies have also reported ^{15}N enrichment in needles of Norway spruce (*Picea abies*) and wheat due to environmental stress (i.e. declining forest and ozone exposure) (Gebauer and Schulze, 1991; Hofmann et al., 1997). It is not clear why wheat and barley exhibited very different responses on N uptake when exposed to CeO_2-NPs. Whether

these differences were due to root structure, nanoparticle dissolution in the root, or physiological changes in plant need to be elucidated in future studies.

4.3 CeO_2-NPs translocation in wheat and barley shoots

The synchrotron micro-XRF analysis showed that both wheat and barley translocated CeO_2-NPs to the shoots regardless of N source in the growth media (Figure 4). We have shown in previous hydroponic studies the uptake of Ce in wheat and barley seedlings (Rico et al., 2015b), which corroborates the plant uptake of CeO_2-NPs recorded in the current study. Our data on speciation is in agreement with data normally reported in the literature regarding the accumulation of CeO_2-NPs in plants grown in hydroponic culture solution (Rico et al., 2013; Spielman-Sun et al., 2017; Zhang et al., 2012). Unfortunately, the data does not allow further speciation analysis to determine which part of the plants the reduction occurred. Our findings also revealed that CeO_2-NPs were translocated to the shoots suggesting an uptake of CeO_2-NPs in barley plants; however, barley seedlings did not exhibit decreases in biomass or ^{15}N uptake (Table 2, Figures 2 and 3). More studies should be performed to understand why CeO_2-NPs markedly disturbed N or ^{15}N uptake in wheat than barley.

5. Conclusion

The goal of this study was to determine if CeO_2-NP exposure altered the uptake or apparent metabolism of N by two commercially important plant species. We used hydroponic culture in order to control the amount, the forms and isotopic composition of N supplied to the plants during exposure. We found that decreases in $\delta^{15}N$ in wheat were due to low assimilation of $(N)_{inorg}$ and efflux of ^{15}N-enriched $(N)_{inorg}$ while increases in $\delta^{15}N$ in barley were probably due to conversion of all $(N)_{inorg}$ to $(N)_{org}$. The study also revealed that root-to-shoot translocation of CeO_2-NPs without negative effects on N and ^{15}N dynamics in barley. Although the longer-term consequences of shifts in isotopic N are unknown, they clearly show the potential for ENMs to interfere with plant metabolism of critical plant nutrients. Additional studies will be needed to determine the extent to which these metabolic changes occur in soils containing intact root-rhizospheres, and also whether these changes lead to shifts in nutrient dynamics in terrestrial ecosystems.

Acknowledgments

The authors would like to thank R. Brooks and W. Rugh for assistance in conducting the stable isotope measurements and for thoughtful discussions regarding the data. We thank S. Perakis for his comments on an earlier version of this manuscript. The information in this document was funded by the U.S. Environmental Protection Agency. It has been subjected to the agency's peer and administrative review, and it has been approved for publication as a U.S. Environmental Protection Agency document. Mention of trade names or commercial products does not constitute endorsement or recommendation for use. The operations at the Advanced Light Source are supported by the Director, Office of Science, Office of Basic Energy Sciences, US Department of Energy under Contract No. DE-AC02–05CH11231.

Appendix

Appendix A.: Nitrogen transport processes in plant

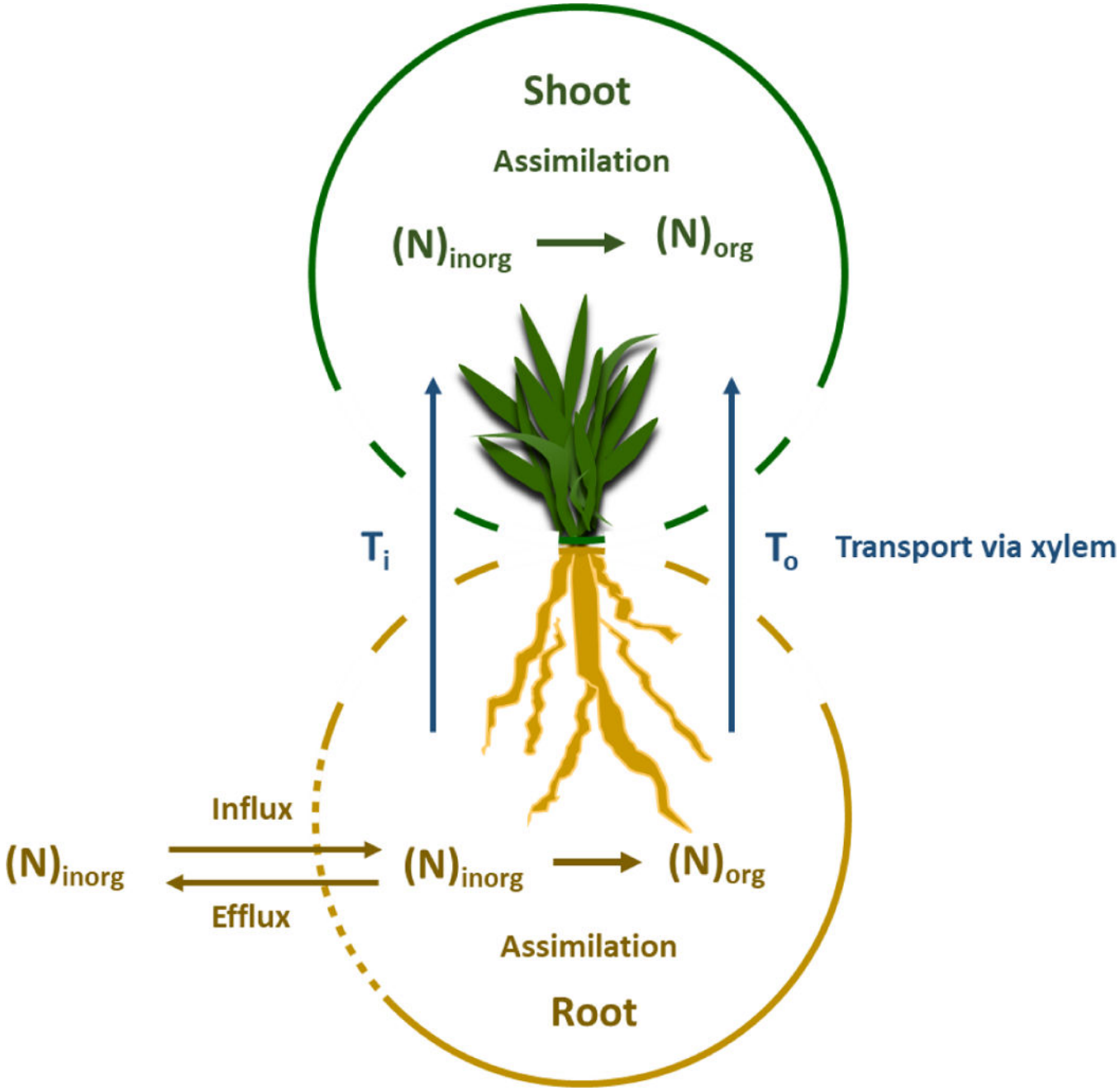

Figure A.1.

Transport processes causing isotopic $\delta^{15}N$ discrimination observed in plants as described in the literature (Kalcsits et al. (2014), copyright license granted by John Wiley and Sons). $(N)_{org}$ = organic N, $(N)_{inorg}$ = inorganic N, T_o = $(N)_{org}$ transport, T_i = $(N)_{inorg}$ transport.

Appendix B.: Synchrotron analysis

Small amounts of these mixtures were sprinkled onto the adhesive side of Kapton tape and covered with another piece of Kapton tape and presented to the μXRF beamline at room temperature. The beam energy was calibrated so that the first peak for CeO_2-NPs was at 5730.39eV. Data were taken with a fine spacing near 5848.6eV, where a monochromator Bragg glitch served as an internal energy calibrant for each spectrum. The short dwell time in this region is the source of the noisiness of all spectra there. Because the white-line intensity is high, the fluorescence spectra for the Ce(III) references are very sensitive to overabsorption ("self-absorption") (Goulon et al., 1981; Manceau et al., 2002). Therefore, we took spectra at places where the intensity was high, for good signal, and at tiny particles, where the spectra were noisy but the same for a range of particles which yielded different count rates. We thus considered that these particles were small enough to avoid overabsorption, and adjusted the spectra from the stronger-signal areas using a simple model for overabsorption with the amount of overabsorption varied so the spectral shapes for the strong-signal areas matched those for the tiny particles. This procedure gives us the signal quality from the strong-signal areas and the freedom from overabsorption found with small particles.

Reference standard XANES spectra for LCF were obtained from Ce(IV) oxide nanoparticles, Ce(III) acetate, Ce(III) carbonate, Ce(III) oxalate, and Ce(III) phosphate. The standards were prepared by blending a 1:1 (w/w) ratio of the standards and boron carbide (B_4C) with a clean agate mortar and pestle. Linear combination fit (LCF) analysis was performed with Ce(III) species standards was performed on their μXANES spectra; however, LCF values obtained were not significantly different from each other that fit from one Ce(III) species was used (Appendix D.1).

Appendix C.: ANOVA of wheat or barley exposed to cerium oxide nanoparticles

Table C.1.

Two-way ANOVA of biomass, N and $\delta^{15}N$ in wheat exposed to cerium oxide nanoparticles.[a]

Treatment	CE	NS	CE×NS
Root biomass	0.0067***	<0.0001****	0.0079***
Shoot biomass	0.0840**	<0.0001****	0.0343**
Root % N	0.5421^{ns}	<0.0001****	0.3352^{ns}
Shoot % N	0.4046^{ns}	0.0003****	0.0956*
Total root N	0.5421^{ns}	<0.0001****	0.3352^{ns}
Total shoot N	0.0723*	0.0009****	0.0090***
Total plant N	0.0127**	<0.0001****	0.0004***
Root $\delta^{15}N$	0.0047***	<0.0001****	0.0004***
Shoot $\delta^{15}N$	0.0920*	<0.0001****	0.6279^{ns}
Whole-plant $\delta^{15}N$	0.0369**	<0.0001****	0.0027***

[a] CeO_2-NPs as the main factor with Ce-0 and Ce-500 as the treatments, NS = N source as another factor composed of NH_4NO_3, NH_4^+, and NO_3^- treatments. Statistical significance at P ≤ 0.10, 0.05, and 0.001 was indicated as *, **, and ***, respectively. ns indicates no significance.

Table C.2.

Two-way ANOVA of biomass, N and $\delta^{15}N$ in barley exposed to cerium oxide nanoparticles.[a]

Treatment	CE	NS	CE×NS
Root biomass	0.1069^{ns}	<0.0001****	0.9286^{ns}
Shoot biomass	0.2457^{ns}	0.0013***	0.8868^{ns}
Root % N	0.0811*	0.1755^{ns}	0.9875^{ns}
Shoot % N	0.4464^{ns}	0.0034***	0.4193^{ns}
Total root N	0.1088^{ns}	<0.0001****	0.4859^{ns}
Total shoot N	0.0344**	<0.0001****	0.3566^{ns}
Total plant N	0.0270**	<0.0001****	0.3316^{ns}
Root $\delta^{15}N$	0.0479**	<0.0001****	0.5821^{ns}
Shoot $\delta^{15}N$	0.2139^{ns}	<0.0001****	0.2435^{ns}
Whole-plant $\delta^{15}N$	0.1138^{ns}	<0.0001****	0.2707^{ns}

[a] CeO_2-NPs as the main factor with Ce-0 and Ce-500 as the treatments, NS = N source as another factor composed of NH_4NO_3, NH_4^+, and NO_3^- treatments. Statistical significance at P ≤ 0.10, 0.05, and 0.001 was indicated as *, **, and ***, respectively. ns indicates no significance.

Appendix D.: Linear combination fits (LCF) analysis

Table D.1.

Linear combination fits of Ce micro-XANES spectra obtained in shoots of wheat and barley exposed to cerium oxide nanoparticles (500 mg/L) for 10 days in hydroponic suspension supplied with different forms of N. NSS is the normalized sum-square error of the fit $\sum(y - y_{fit})^2 / \sum y^2$ where y and y_{fit} are the XANES spectrum and fit, respectively.

N treatment	Plant	Ce LCF analysis	NSS
NH_4NO_3	Wheat	80.91% CeO_2 NPs + 18.94% Ce(III)	0.000206
	Barley	92.41% CeO_2 NPs + 6.65% Ce(III)	0.000311
NH_4^+	Wheat	88.28% CeO_2 NPs + 11.98% Ce(III)	0.000123
	Barley	88.12% CeO_2 NPs + 12.18% Ce(III)	0.000285
NO_3^-	Wheat	92.65% CeO_2 NPs + 7.32% Ce(III)	0.001725
	Barley	91.89% CeO_2 NPs + 7.99% Ce(III)	0.000366

References

Ariz I, Cruz C, Neves T, Irigoyen JJ, Garcia-Olaverri C, Nogues S, Aparicio-Tejo PM, Aranjuelo I, 2015 Leaf $\delta^{15}N$ as a physiological indicator of the responsiveness of N_2-fixing alfalfa plants to elevated [CO_2], temperature and low water availability. Frontiers Plant Sci. 6, 574–584.

Banas D, Vollaire Y, Danger M, Thomas M, Oliveira-Ribeiro CA, Roche H, Ledore Y, 2009 Can we use stable isotopes for ecotoxicological studies? Effect of DDT on isotopic fractionation in *Perca fluviatilis*. Chemosphere 76, 734–739. [PubMed: 19576618]

Craine JM, Brookshire ENJ, Cramer MD, Hasselquis NJ, Koba K, Marin-Spiotta R, Wang L, 2015 Ecological interpretations of nitrogen isotope ratios of terrestrial plants and soils. Plant Soil 396, 1–26.

Dahle JT, Arai Y, 2015 Environmental geochemistry of cerium: Applications and toxicology of cerium oxide nanoparticles. Int. J. Environ. Res. Public Health 12, 1253–1278. [PubMed: 25625406]

Evans RD, 2001 Physiological mechanisms influencing plant nitrogen isotope composition. Trends Plant Sci. 6, 121–126. [PubMed: 11239611]

Evans RD, Bloom AJ, Sukrapanna SS, Ehleginger JR, 1996 Nitrogen isotope composition to tomato (*Lycopersicon Esculentum* Mill. Cv. T-5) grown under ammonium or nitrate nutrition. Plant Cell Environ. 19, 1317–1323.

Freeman JL, Zhang LH, Marcus MA, Fakra S, McGrath SP, Pilon-Smits EAH, 2006 Spatial imaging, speciation, and quantification of selenium in the hyperaccumulator plants *Astragalus bisulcatus* and *Stanleya pinnata*. Plant Physiol. 142, 124–134. [PubMed: 16920881]

Gebauer G, Schulze ED, 1991 Carbon and nitrogen isotope ratios in different compartments of a healthy and declining *Picea abies* forest in the Fichtelgebirge, NE Bavaria. Oecologia 87, 198–207. [PubMed: 28313836]

Hofmann D, Jung K, Bender J, Gehre M, Schuurmann G, 1997 Using natural isotope variations of nitrogen in plants as an early indicator of air pollution stress. J. Mass Spectrom. 32, 855–863.

Kalcsits LA, Buschhaus HA, Guy RD, 2014 Nitrogen isotope discrimination as an integrated measure of nitrogen fluxes, assimilation and allocation in plants. Physiol. Plantarum. 151, 293–304.

Kalcsits LA, Guy RD, 2013 Whole-plant and organ-level nitrogen isotope discrimination indicates modification of partitioning of assimilation, fluxes and allocation of nitrogen in knockout lines of *Arabidopsis Thaliana*. Physiol. Plantarum 149, 249–259.

Keller AA, Wang H, Zhou D, Lenihan HS, Cherr G, Cardinale BJ, Miller R, Ji Z, 2010 Stability and aggregation of metal oxide nanoparticles in natural aqueous media. Environ. Sci. Technol. 44, 1962–1967. [PubMed: 20151631]

Manceau A, Marcus MA, Tamura N, 2002 “Quantitative speciation of heavy metals in soils and sediments by synchrotron X-ray techniques”, in Applications of Synchrotron Radiation in Low-Temperature Geochemistry and Environmental Science, Fenter P and Sturchio NC, Eds.Reviews in Mineralogy and Geochemistry, Mineralogical Society of America, Washington, DC., 49, 341–428.

Mariotti A, Mariotti F, Champigny ML, Amarger N, Moyse A, 1982 Nitrogen isotope fractionation associated with nitrate reductase activity and uptake of NO3- by pearl millet. Plant Physiol. 69, 880–884. [PubMed: 16662313]

Marshall JD, Brooks JR, and Lajtha K, 2007 Sources of variation in the stable isotopic composition of plants In Stable isotopes in Ecology and Environmental Science, Michener R and Lajtha K, Eds., Blackwell Publishing, Malden, MA, pgs. 22–60.

Rico CM, Barrios AC, Tan W, Rubenecia R, Lee SC, Varela-Ramirez A, Peralta-Videa JR, Gardea-Torresdey JL, 2015a Physiological and biochemical response of soil-grown barley (*Hordeum vulgare* L.) to cerium oxide nanoparticles. Environ. Sci. Pollut. Res. 22, 10551–10558.

Rico CM, Johnson MG, Marcus MA, Andersen CP, 2017 Intergenerational responses of wheat (*Triticum Aestivum* L.) to cerium oxide nanoparticles exposure. Environ. Sci. Nano 4, 700–711. [PubMed: 30147938]

Rico CM, Johnson MG, Marcus MA, 2018 Cerium oxide nanoparticles transformation at the root-soil interface of barley (*Hordeum vulgare* L.). Environ. Sci. Nano DOI:10.1039/C8EN00316E

Rico CM, Lee SC, Rubenecia R, Mukherjee A, Hong J, Peralta-Videa JR, Gardea-Torresdey JL, 2014 Cerium oxide nanoparticles impact yield and modify nutritional parameters in wheat (*Triticum aestivum* L.). J. Agric. Food Chem. 62, 9669–9675. [PubMed: 25220448]

Rico CM, Morales MI, McCreary R, Castillo-Michel H, Barrios AC, Hong J, Tafoya A, Lee WY, Varela-Ramirez A, Peralta-Videa JR, Gardea-Torresdey JL, 2013 Cerium oxide nanoparticles modify the antioxidative stress enzyme activities and macromolecule composition in rice seedlings. Environ. Sci. Technol. 47, 14110–14008. [PubMed: 24266714]

Rico CM, Peralta-Videa JR, Gardea-Torresdey JL, 2015b Differential effects of cerium oxide nanoparticles on rice, wheat, and barley roots: A fourier transform infrared (FT-IR) microspectroscopy study. Appl. Spectrosc. 69, 287–295. [PubMed: 25587938]

Robinson D, Handley LL, Scrimgeour CM, Gordon DC, Forster BP, Ellis RP, 2000 Using stable isotope natural abundances ($\delta^{15}N$ and $\delta^{13}C$) to integrate the stress responses of wild barley (*Hordeum Spontaneum* C. Koch.) genotypes. J. Exp. Bot. 51, 41–50. [PubMed: 10938794]

Schmidt AC, Reisser W, Mattusch J, Wennrich R, Jung K, 2004 Analysis of arsenic species accumulation by plants and the influence on their nitrogen uptake. J. Anal. At. Spectrom. 19, 172–177.

Servin AD, White JC, 2016 Nanotechnology in agriculture: Next steps for understanding engineered nanoparticle exposure and risk. NanoImpact 1, 9–12.

Spielman-Sun E, Lombi E, Donner E, Howard D, Unrine JM, Lowry GV, 2017 Impact of surface charge on cerium oxide nanoparticle uptake and translocation by wheat (*Triticum Aestivum*). Environ. Sci. Technol. 51, 7361–7368. [PubMed: 28575574]

Sutter K, Jung K, Krauss GJ, 2002 Effects Of heavy metals on the nitrogen metabolism of the aquatic moss *Fontnalis Antipyretica* L. Ex Hedw. - A ^{15}N tracer study. Environ. Sci. Pollut. Res 9, 417–421.

Tamm CO, 1991, Nitrogen in Terrestrial Ecosystems: Questions of productivity, vegetational changes, and ecosystem stability Ecological Studies 81, Springer-Verlag Berlin Heidelberg, DOI: 10.1007/978-3-642-75168-4.

Unkovich M, 2013 Isotope discrimination provides new insight into biological nitrogen fixation. New Phytol. 198, 643–646. [PubMed: 23461709]

Yoshida S, Forno DA, Cock JH, Gomez KA, 1976 Laboratory Manual for Physiological Studies of Rice; International Rice Research Institute: Los Baños, Laguna, Philippines.

Zhang P, Ma Y, Zhang Z, He X, Zhang J, Guo Z, Tai R, Zhao Y, Chai Z, 2012 Biotransformation of ceria nanoparticles in cucumber plants. ACS Nano 6, 9943–9950. [PubMed: 23098040]

Zuverza-Mena N, Martinez-Fernandez D, Du W, Hernandez-Viezcas JA, Bonilla-Bird N, Lopez-Moreno ML, Komarek M, Peralta-Videa JR, Gardea-Torresdey JL, 2017 Exposure of engineered nanomaterials to plants: Insights into the physiological and biochemical responses – A review. Plant Physiol. Biochem. 110, 236–264. [PubMed: 27289187]

Goulon J; Goulon-Ginet C; Cortes R; Dubois JM On experimental attenuation factors of the amplitude of the EXAFS oscillations in absorption, reflectivity and luminescence measurements. J. Phys. 1981, 42, 539–548.

Manceau A; Marcus MA; Tamura N (2002) “Quantitative speciation of heavy metals in soils and sediments by synchrotron X-ray techniques”, in Applications of Synchrotron Radiation in Low-Temperature Geochemistry and Environmental Science, Fenter P and Sturchio NC, Eds.Reviews in Mineralogy and Geochemistry, Mineralogical Society of America, Washington, DC., 49, 341–428.

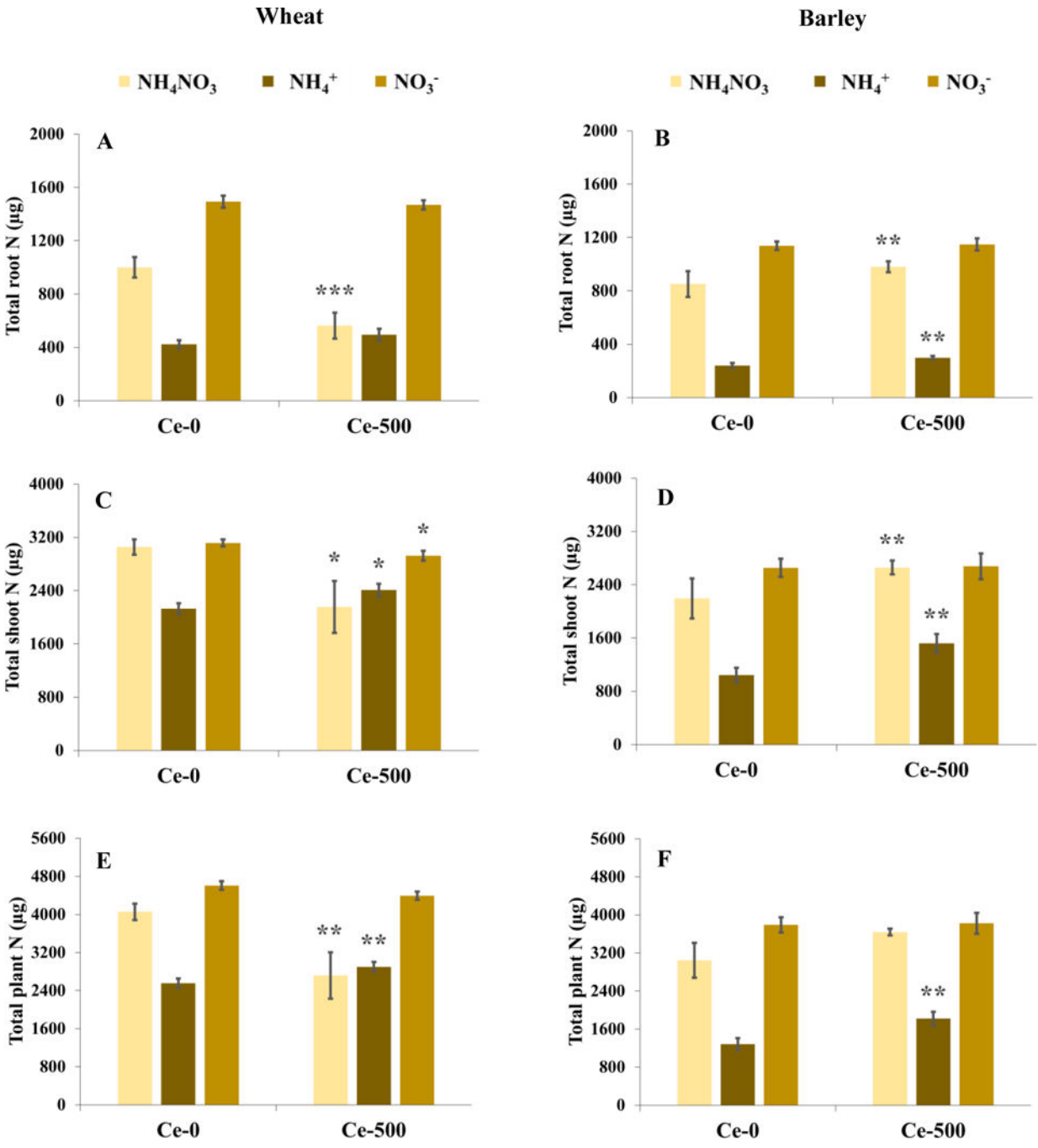

Figure 1.

N contents in wheat and barley exposed to CeO_2-NPs in hydroponic solutions with different N sources. Ce-0 = 0 mg CeO_2-NPs/L, Ce-500 = 500 mg CeO_2-NPs/L. Values are means ± SE (n = 6). Statistical difference between Ce-0 and Ce-500 at P ≤ 0.10, 0.05, and 0.01 between Ce-0 and Ce-500 treatments was indicated as *, **, and ***, respectively.

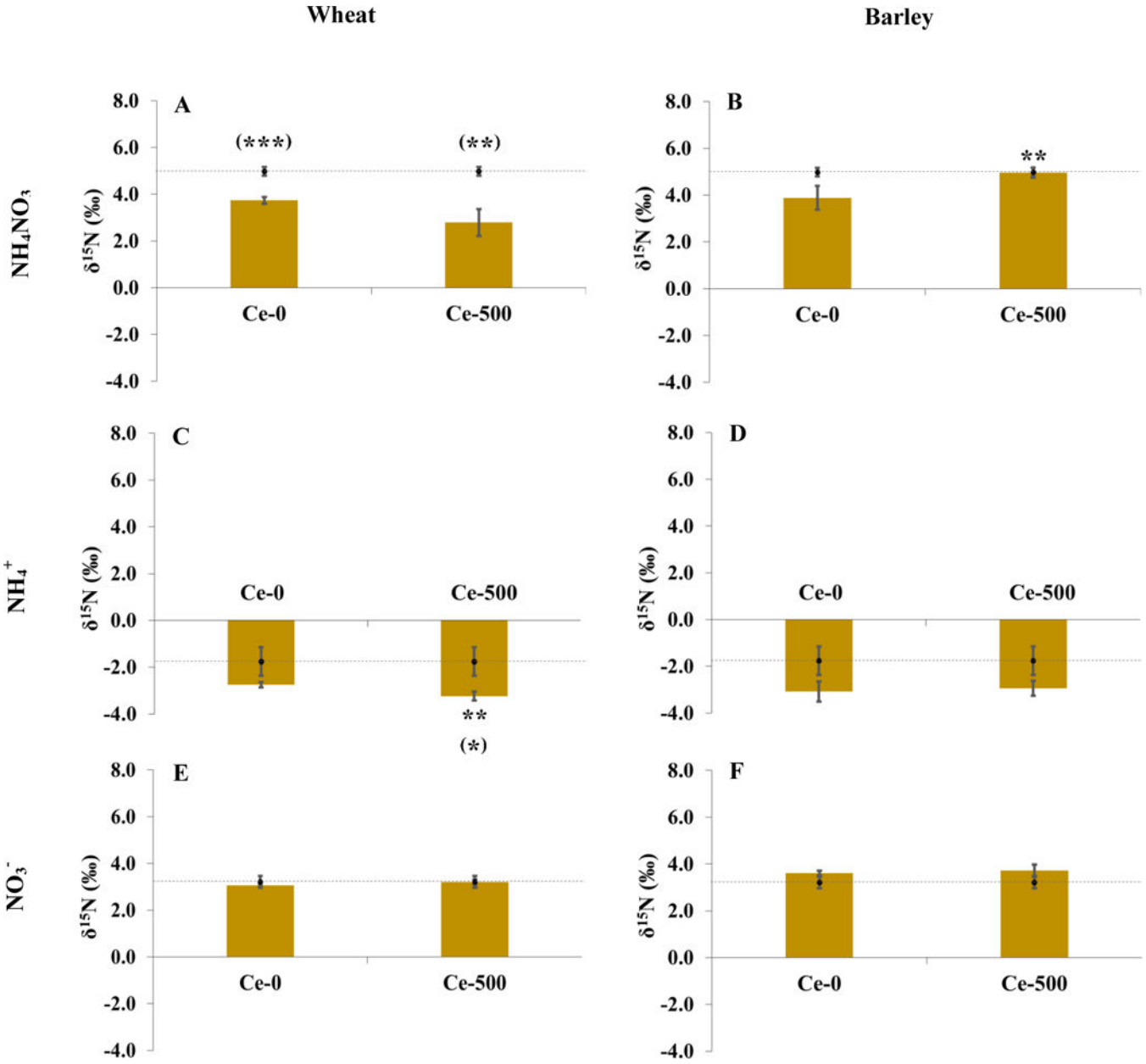

Figure 2.

Whole-plant $\delta^{15}N$ of wheat and barley exposed to CeO_2-NPs in hydroponic solutions with different N sources. Ce-0 = 0 mg CeO_2-NPs/L, Ce-500 = 500 mg CeO_2-NPs/L. Values are means ± SE (n = 6). Statistical difference between Ce-0 and Ce-500 at P ≤ 0.10, 0.05, and 0.01 between Ce-0 and Ce-500 treatments was indicated as *, **, and ***, respectively. Labels outside the bar indicates differences in $\delta^{15}N$ between CeO_2-NPs while in labels in parenthesis indicates differences in $\delta^{15}N$ between CeO_2-NPs treatment and N source. Dashed lines indicate the $\delta^{15}N$ of the N source.

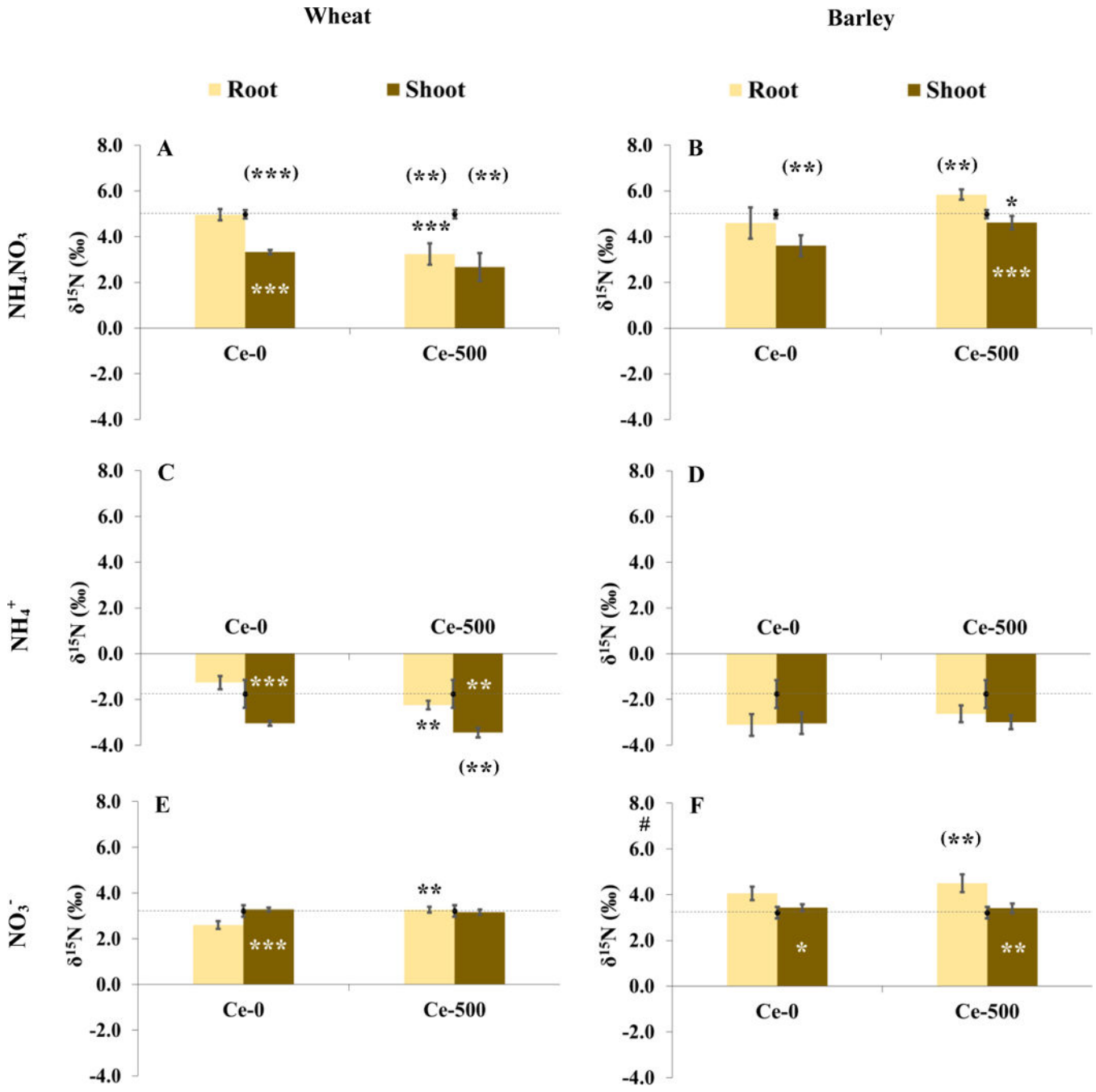

Figure 3.

Isotopic $\delta^{15}N$ of wheat and barley exposed to CeO_2-NPs in hydroponic solutions with different N sources. Ce-0 = 0 mg CeO_2-NPs/L, Ce-500 = 500 mg CeO_2-NPs/L. Values are means ± SE (n = 6). Statistical difference between Ce-0 and Ce-500 at P ≤ 0.10, 0.05, and 0.01 was indicated as *, **, and ***, respectively. Labels outside the bar indicates differences in $\delta^{15}N$ between CeO_2-NPs while in labels in parenthesis indicates differences in $\delta^{15}N$ between CeO_2-NPs treatment and N source. Dashed lines indicate the $\delta^{15}N$ of the N source.

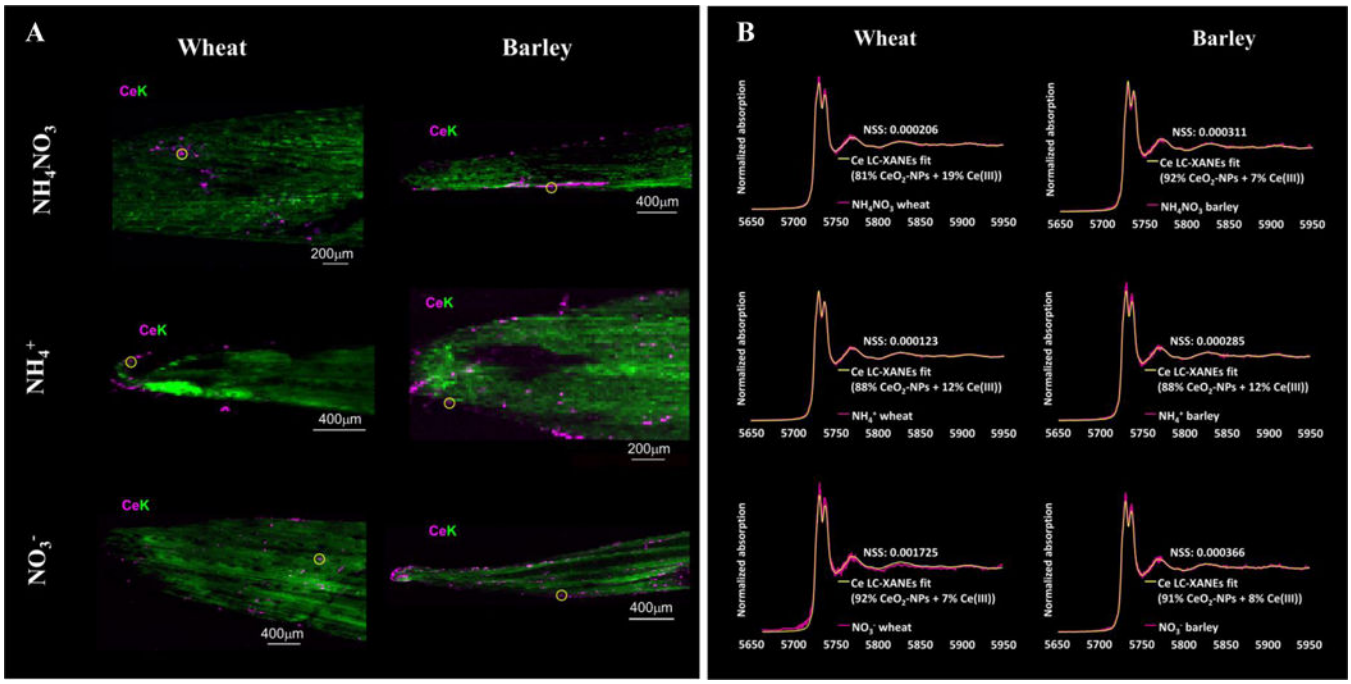

Figure 4.

Synchrotron micro-X-ray fluorescence analysis of wheat and barley exposed to CeO_2-NPs at different N sources. (A) Bicolor micro-XRF maps of wheat and barley shoots (magenta = Ce, green = K). (B) Ce micro-XANES spectra from spots on shoots. Spectra on magenta line represents linear combination fits and yellow solid line spectra represents μXANES from the sample. The range of values in Ce(III) are from Ce(III) acetate, Ce(III) carbonate, Ce(III) oxalate, and Ce(III) phosphate. Exact values are given in Table D.1.

Table 1.

Global mean (mean across different N sources) N and $\delta^{15}N$ of wheat and barley exposed to cerium oxide nanoparticles for 10 days in hydroponic suspension supplied with different forms of N. Values are mean ± SE (*n = 18*).[a]

Global mean	Wheat		Barley	
	Ce-0	Ce-500	Ce-0	Ce-500
Root biomass (mg)	45 ± 7	37 ± 6***	23 ± 4	27 ± 4
Shoot biomass (mg)	106 ± 6	96 ± 5*	67 ± 6	76 ± 6
Root N (%)	2.40 ± 0.09	2.43 ± 0.07	3.51 ± 0.19	3.09 ± 0.14*
Shoot N (%)	2.64 ± 0.05	2.58 ± 0.09	2.95 ± 0.16	3.09 ± 0.14
Root N (μg)	973 ± 110	842 ± 113**	743 ± 96	809 ± 91
Shoot N (μg)	2766 ± 119	2595 ± 150*	1964 ± 197	2285 ± 155**
Plant N (μg)	3739 ± 221	3337 ± 241**	2707 ± 287	3094 ± 235**
Root $\delta^{15}N$ (‰)	2.10 ± 0.64	1.42 ± 0.65***	1.85 ± 0.90	2.57 ± 0.92**
Shoot $\delta^{15}N$ (‰)	1.19 ± 0.73	0.80 ± 0.76*	1.33 ± 0.78	1.68 ± 0.82
Whole-plant $\delta^{15}N$ (‰)	1.35 ± 0.71	0.92 ± 0.74*	1.47 ± 0.81	1.92 ± 0.85

[a]Ce-0 and Ce-500 were 0 and 500 mg CeO_2-NPs/L. Statistical difference between Ce-0 and Ce-500 at $P \leq 0.10$, 0.05, and 0.01 was indicated as *, **, and ***, respectively.

Table 2.

Biomass and N concentration of wheat and barley exposed to cerium oxide nanoparticles for 10 days in hydroponic suspension supplied with different forms of N. Values are mean ± SE ($n = 6$).[a]

	Wheat		Barley	
	Ce-0	**Ce-500**	**Ce-0**	**Ce-500**
NH_4NO_3				
Root biomass (mg)	40 ± 4	22 ± 3***	24 ± 5	29 ± 2
Shoot biomass (mg)	123 ± 8	95 ± 12*	70 ± 11	83 ± 10
Root N concentration (%)	2.51 ± 0.08	2.49 ± 0.07	3.80 ± 0.31	3.43 ± 0.28
Shoot N concentration (%)	2.52 ± 0.09	2.20 ± 0.17	3.20 ± 0.23	3.36 ± 0.28
NH_4^+				
Root biomass (mg)	16 ± 1	18 ± 2	7 ± 1	10 ± 1***
Shoot biomass (mg)	77 ± 3	86 ± 4	46 ± 5	55 ± 5
Root N concentration (%)	2.74 ± 0.02	2.71 ± 0.05	3.38 ± 0.22	2.93 ± 0.05*
Shoot N concentration (%)	2.78 ± 0.06	2.81 ± 0.07	2.31 ± 0.12	2.75 ± 0.16**
NO_3^-				
Root biomass (mg)	78 ± 4	71 ± 3	37 ± 5	41 ± 4
Shoot biomass (mg)	119 ± 4	108 ± 5	84 ± 11	89 ± 11
Root N concentration (%)	1.93 ± 0.07	2.09 ± 0.09	3.35 ± 0.43	2.91 ± 0.28
Shoot N concentration (%)	2.63 ± 0.07	2.72 ± 0.06	3.33 ± 0.28	3.16 ± 0.24

[a]Ce-0 and Ce-500 were 0 and 500 mg CeO_2-NPs/L. Statistical difference between Ce-0 and Ce-500 at $P \leq 0.10$, 0.05, and 0.01 was indicated as *, **, and ***, respectively.